

42(1), pp. 11-18, 2014

DOI: [10.3311/PPtr.7062](https://doi.org/10.3311/PPtr.7062)

<http://www.pp.bme.hu/tr/article/view/7062>

Creative Commons Attribution 

Péter Bauer

RESEARCH ARTICLE

RECEIVED 4 OCTOBER 2013; ACCEPTED 13 JANUARY 2014

Abstract

The paper presents and evaluates the simple simulation of the landing gear used in small unmanned aerial vehicles (UAVs). The main goal was to set up software-in-the-loop (SIL) and hardware-in-the-loop (HIL) simulation environments that can be used in testing flight control and flight estimation algorithms from take-off to landing. Small UAVs without gear braking were considered in the study, the stopping of aircraft was due solely to frictional forces. The model developed can be used in simulations to describe aircraft motion from standstill on the ground through take-off to landing and stoppage. The parameters were tuned experimentally for each small UAV type. Finally, SIL simulation results are presented and evaluated in the paper.

Keywords

Landing gear · unmanned aerial vehicle simulation · simple model · from take-off to landing

1 Introduction

SIL and HIL simulation environments are crucial in the testing of control algorithms. In ground vehicle modelling the inclusion of the model of wheel-surface interaction is mandatory, because it highly affects the dynamics of the vehicle (see Nagy, Gáspár, 2012; Németh, Gáspár, 2010). However, the inclusion of landing gear ground effects in an aircraft HIL simulation environment can be missing, see for example (Paw, 2009) and (Jung, Tsiotras, 2007). This arises the need to integrate a landing gear model into such simulations to appropriately model the take-off and landing considering also the start and stop of taxiing on the ground.

In this work only small UAVs without braking system and with non-retractable landing gears are considered. This means the requirement to model the stopping of aircraft purely with friction forces. Of course the stiffness and damping of landing gear should be also modelled. The steering of wheel(s) is also not considered, because in simulation it is not very important to correctly taxi the plane on ground.

In (Denery et al., 2006) the landing gear model is integrated into the HIL simulation by considering only the normal and lateral forces, without rolling resistance. Simulation results with stopping vehicle are not presented. (Abdunabi, 2006) includes stiffness, damping, static, rolling and dynamic friction separately for every wheel on the aircraft. A detailed calculation model can be found in (jsbsim groundreactions). The separate consideration of wheels can be too complicated in the modelling of a small UAV if the goal is not the sizing of the landing gear.

Other sources (Khapane, 2007; Dassault Systèmes SIMULIA, 2010; Barnes, Yager, 1985; Lyle et al. 2002; Li et al., 2012; Verzichelli, 2008; Lernbeiss, Ploechl, 2007; Kargin, 2007; Miranda de Almeida, 2007) publish different models with simpler or more complicated structures, but the stopping of aircraft is included only by brake application and the technical details are usually missing.

That's why the goal of this work is to develop a landing gear model which is as simple as possible but includes all of the crucial characteristics (only to generate data similar to

Péter Bauer

Department of Control for Transportation and Vehicle Systems,

Budapest University of Technology and Economics,

Stoczek u. 2., H-1111 Budapest, Hungary

Institute for Computer Science and Control, Hungarian Academy of Sciences

e-mail: bauer.peter@mail.bme.hu

real flight). In the following, the step by step development of the model will be presented and finally illustrated with SIL simulation results. The example is the E-flite Ultrastick 25e tail gear aircraft, but the method can be applied to nose gear and other aircraft versions also. The original SIL and HIL simulations of this aircraft were developed in (Paw, 2009) without landing gear modelling. The aircraft can be seen in figure 1.

2 The landing geometry of the aircraft

The basic concept of the modelling of landing gear (two main and one tail wheel) is to neglect the separate effects of the wheels and substitute the vertical part with a single spring and damper along the Z axis (a 'rod' below the fuselage incorporating the stiffness and damping of landing gear mechanics and tire) and a torsional spring and damper around the Z axis. The pitching and banking effects are simulated with torsional springs and dampers along the X and Y axes (see figure 2). The X-Y-Z body coordinate system is rotated with θ_0 around the Y body axis to be aligned with the ground (X axis parallel to ground, Z axis perpendicular) see figure 3. This means alignment with the earth coordinate system.

From the viewpoint of geometry, first the ground touching of the virtual rod should be detected. The initial compressed length and the initial pitch angle of the aircraft (A/C) can be calculated based-on figure 3. Zero roll angle is assumed, and the yaw angle has no influence on ground forces and moments (flat earth model is considered).

In the figure v_1, v_2, v_3 are the vectors pointing from aircraft center of gravity (CG) to the ground touching points in body coordinate system (coord. sys.).

The initial θ_0 pitch angle relative to the ground can be calculated as follows:

$$\begin{aligned} v_{1p} &= [v_1(x) \quad v_1(z)]^T \\ v_{3p} &= [v_3(x) \quad v_3(z)]^T \\ dv &= v_{1p} - v_{3p} = [dx \quad dz]^T \\ \theta_0 &= \arctg\left(\frac{dz}{dx}\right) \end{aligned} \quad (1)$$

Note: from now on, the X, Y, and Z coordinate of a vector is denoted by (x), (y) and (z).

The initial CG height above the ground (compressed virtual rod length) can be calculated as follows:

$$\begin{aligned} \alpha &= \arctg\left(\frac{v_1(z)}{v_1(x)}\right) \\ h_0 &= \sqrt{v_1^2(x) + v_1^2(z)} \cdot \sin(\alpha - \theta_0) \end{aligned} \quad (2)$$

From this data the compression of the spring-damper system and the pitch and bank angles relative to the steady position on ground can be later calculated. The former from the altitude of A/C CG above ground.



Fig. 1. The E-flite Ultrastick 25e aircraft

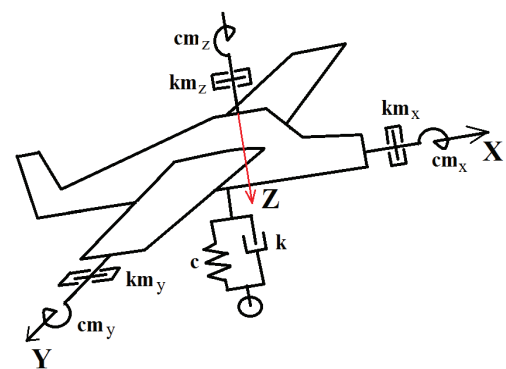


Fig. 2. The basic model structure

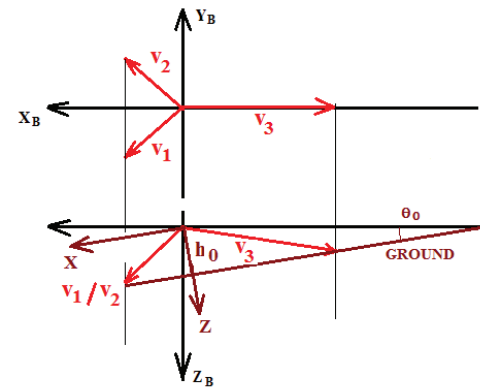


Fig. 3. Wheel position vectors in aircraft body coordinate system

The compression length of the spring-damper system when the A/C rests on the ground can be calculated considering aircraft mass m and virtual rod stiffness c :

$$dl_0 = \frac{m \cdot g}{c}$$

here g is the gravitational constant.

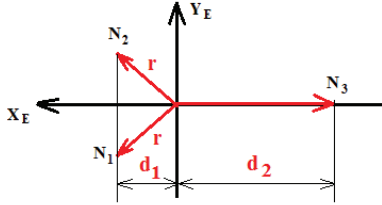


Fig. 4. Yaw motion in earth coord. sys.

Considering the yawing motion, the rotation around the Z axis means that the three wheels are sliding on the ground (the rolling of wheels is neglected in this case). If the aircraft has nonzero yaw rate the yaw moment is modelled with a saturated torsional damper. If the yaw rate is zero the potential yaw moment can be calculated from the static friction of aircraft. So, it can be assumed that all three wheels are on the ground and the A/C is in equilibrium considering the vertical forces and their moments during the calculation of the potential yaw moment from static friction. The separate effect of the three wheels can be unified in a yaw moment fictitious arm considering the static friction coefficient and normal force as follows.

Denote the total normal force (in the Z direction of earth coord. sys.) with F_N and its absolute value with N , while its components on the wheels with N_1 , N_2 and N_3 .

From the vertical force and X and Y moment equilibrium the normal force components can be first calculated considering the wheel geometry in figure 4 (r , d_1 and d_2 can be calculated from v_1 , v_2 , v_3 by first transforming them into earth coord. sys. with θ_0) as shown below.

$$\begin{aligned}
 N_1 &= N_2 \quad X \text{ moment equilibrium} \\
 (N_1 + N_2)d_1 &= N_3d_2 \quad Y \text{ moment equilibrium} \\
 N_1 + N_2 + N_3 &= N \quad Z \text{ force equilibrium} \\
 2N_1d_1 &= N_3d_2 \Rightarrow N_3 = \frac{2d_1N_1}{d_2} \\
 2N_1 + \frac{2d_1N_1}{d_2} &= N = \frac{2(d_1+d_2)}{d_2} N_1 \Rightarrow \\
 N_1 = N_2 &= \frac{d_2}{2(d_1+d_2)} N \quad N_3 = \frac{d_1}{d_1+d_2} N
 \end{aligned} \tag{3}$$

It is assumed that the friction forces are perpendicular to r -s and d_2 when the aircraft rotates. Assuming a positive yaw moment from friction forces and considering μ_s as the static friction coefficient the following equation results (of course,

during the calculations later the sign of yaw moment depends on the rotational direction of the aircraft):

$$\begin{aligned}
 M_{z_1} &= (rN_1 + rN_2 + d_2N_3)\mu_s = \\
 &= \left(\frac{2r \cdot d_2}{2(d_1+d_2)} N + \frac{d_1d_2}{d_1+d_2} N \right) \mu_s = \\
 &= \underbrace{\left(\frac{r \cdot d_2 + d_1d_2}{d_1+d_2} \right)}_{cm_z} \mu_s N
 \end{aligned} \tag{4}$$

Here, cm_z is the fictitious arm with which the yaw moment can be calculated from the normal force and the static friction coefficient.

3 The steps of the force and moment calculation

In the following, the steps of the ground (wheel) force and moment calculations will be explained in detail.

STEP 1: Check if the aircraft touches the ground or not, considering actual CG height (h) above ground and h_0 and dl_0 . If $h > h_0 + dl_0$ the aircraft does not touch the ground and so no forces and moments act on the aircraft from ground ($h_0 + dl_0$ is the total undeformed length of the vertical 'spring'). Of course, this is again an approximation because one wheel can touch the ground even if CG is higher than $h_0 + dl_0$. If ground touching is detected the further steps are evaluated.

STEP 2: Calculate the actual body to earth transformation matrix from the Euler angles without considering the ψ yaw angle (the ground forces and moments do not depend on the horizontal orientation of the aircraft in the applied flat earth model):

$$T_{EB} = T_\theta^T T_\phi^T$$

STEP 3: Define the vector of the virtual rod in body coord. sys. From Figure 3 this vector is:

$$v_r^B = [-\sin(\theta_0) \quad 0 \quad \cos(\theta_0)]^T$$

Transform this vector into earth coord. sys.:

$$v_r^E = T_{EB} v_r^B$$

STEP 4: Calculate the roll and pitch angles from v_r^E . These are the deviation angles from the equilibrium (when aircraft rests on the ground) and so, the roll (X) and pitch (Y) moments will be calculated from them. They are calculated similarly to

the angle of attack and angle of sideslip without using trigonometrical functions to simplify calculations:

$$\theta^E = \frac{v_r^E(x)}{v_r^E(z)} \quad (5)$$

$$\phi^E = \frac{-v_r^E(y)}{\sqrt{v_r^E(x)^2 + v_r^E(z)^2}}$$

STEP 5: Transform aircraft velocity and angular velocity vectors into earth coord. sys. (without ψ effect):

$$V^E = T_{EB} V^B \quad (6)$$

$$\omega^E = T_{EB} \omega^B$$

STEP 6: Calculate normal (vertical) ground force vector and its absolute value $N = \|F_N\|$:

$$F_N = \begin{bmatrix} 0 & 0 & -c(h_0 + dl_0 - h) - k \cdot V^E(z) \end{bmatrix}$$

STEP 7: Transform aircraft body force and moment vectors into earth coord. sys. (without ψ effect). These forces and moments include aerodynamic, thrust and gravitational forces and moments (all forces and moments except for ground).

$$F^E = T_{EB} F^B \quad (7)$$

$$M^E = T_{EB} M^B$$

STEP 8: Calculate the direction of rolling forces in earth coord. sys. The axles of the wheels are perpendicular to the XZ plane of body coord. sys. that's why the rolling forces can act only parallel with the body XZ plane, and they should act also parallel to the Earth XY plane. This way the direction of the intersection line between the body XZ and earth XY planes gives the direction of the rolling forces.

The equation of a plane given by its normal vector is as follows:

$$n_x \cdot x + n_y \cdot y + n_z \cdot z + C = 0$$

Here, n_x, n_y, n_z are the coordinates of the normal vector and C is a parameter calculated from a point on which the plane goes through. If the plane goes through the (0,0,0) point C should be 0.

Using the above equation the body XZ and the earth XY planes can be described. The normal vector of body XZ plane is $n^B = [0 \ 1 \ 0]^T$ in the body coord. sys. In Earth coord. sys. it is $n^E = T_{EB} \cdot n^B = [\sin \phi \sin \theta \ \cos \phi \ \sin \phi \cos \theta]^T$.

The normal vector of earth XY plane (in earth coord. sys.) is $n_{xy} = [0 \ 0 \ 1]^T$. All two planes are assumed to go through the (0,0,0) point (so C would be zero for all two planes) without loss of generality because the A/C position relative to earth coord. sys. does not affect the calculations.

A vector in earth XY plane should be obtained which is also in the body XZ plane. Denote this vector by $v_{xy} = [a \ b \ 0]^T$

(in earth coord. sys.). It should be a unit vector to not to scale the forces later. From this we have two constraints for the two unknowns a and b :

- ❶ Unit vector: $a^2 + b^2 = 1$
- ❷ From the body XZ plane equation: $\sin \phi \sin \theta \cdot a + \cos \phi \cdot b = 0$

From these two equations the solutions for a and b are the following:

$$b^2 = 1 - a^2$$

$$\sin \phi \sin \theta \cdot a = -\cos \phi \cdot b$$

$$\sin^2 \phi \sin^2 \theta \cdot a^2 = \cos^2 \phi \cdot b^2 = \cos^2 \phi (1 - a^2)$$

$$(\sin^2 \phi \sin^2 \theta + \cos^2 \phi) a^2 = \cos^2 \phi \quad (8)$$

$$a = -\text{ssign}(F^E(x)) \sqrt{\frac{\cos^2 \phi}{\sin^2 \phi \sin^2 \theta + \cos^2 \phi}}$$

$$b = \sqrt{1 - a^2}$$

if $\text{sign}(ab) \neq -\text{sign}(\phi) \text{sign}(\theta)$: $b = -b$

The last examination should be done because of the second order equation. Sometimes its other (negative) solution is required. The *ssign* is a special function which gives 1 for zero input (not zero). This sign term is required to consider the direction of the $F^E(x)$ body force on the aircraft, because the rolling friction should act in the opposite direction.

STEP 9: Assume, the aircraft rests on the ground. Calculate the ground forces and moments required for aircraft equilibrium, considering the acting forces on the aircraft.

At first, the unified rolling and sliding friction forces are calculated approximately, considering the direction vector v_{xy} and the $F^E(x)$ and $F^E(y)$ forces in earth coord. sys. The used notations can be seen in figure 5. Note that in reality the F_r rolling and F_s sliding forces are acting in the opposite direction of $F^E(x)$ and $F^E(y)$ forces, but the figure is easier to understand this way (equations are written using the correct directions).

From Figure 5 the $F^E(x)$ and $F^E(y)$ forces can be represented by the rolling F_r and sliding F_s friction forces (considering the v_{xy} direction unit vector and the opposite direction of friction forces):

$$F^E(x) = -F_r a + F_s b$$

$$F^E(y) = -F_r b - F_s a$$

$$F_r = \mu_r N$$

$$F_s = \mu N \quad (9)$$

$$\frac{F^E(x)}{N} = -\mu_r a + \mu b$$

$$\frac{F^E(y)}{N} = -\mu_r b - \mu a$$

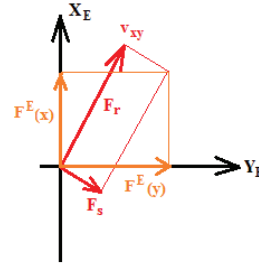


Fig. 5. Notations used in rolling and sliding friction calculations

From the above system of equations it is easy to calculate F_r and F_s from $F^E(x)$ and $F^E(y)$, but there is a limitation. The frictional forces are limited by the N normal force and the friction coefficients and simply solving the system of equations makes the satisfaction of this limitation difficult. That's why an approximate solution is calculated considering the fact that a should be close to 1 and b should be close to zero. The ψ yaw angle was not considered in body to earth transformation, and so body X axis is parallel with the earth X axis if A/C pitch (θ) and roll (ϕ) are zero. This way, only the tilt of the aircraft causes $a \neq 1$ and $b \neq 0$. Assuming small tilt angles, the approximation will be acceptable.

From the first equation (assuming $b = 0$):

$$\mu'_r \approx \frac{-F^E(x)}{aN} \quad \mu'_r = \frac{\mu'_r}{|\mu'_r|} \mu_r$$

This way the signed rolling friction coefficient μ'_r required for the equilibrium is calculated. Of course μ'_r should not exceed μ_r the given maximum coefficient, this is achieved by the normalization.

From the second equation (assuming $a = 1$):

$$\mu' \approx \frac{-F^E(y)}{N} - \mu'_r b \quad \mu' = \frac{\mu'}{|\mu'|} \mu$$

Here, μ' is also limited by the maximum sliding friction coefficient μ . Substituting μ'_r and μ' into

$\frac{F_E(x)}{N}$ and $\frac{F_E(y)}{N}$ we get:

$$\begin{aligned} \frac{F^E(x)}{N} &= -\frac{F^E(x)}{aN} a + \frac{F^E(y)}{N} b - \frac{F^E(x)}{aN} b^2 \\ \frac{F^E(y)}{N} &= \frac{F^E(y)}{N} a - \frac{F^E(x)}{aN} ab + \frac{F^E(x)}{aN} b \end{aligned} \quad (10)$$

The above two equations show that if $a = 1$ and $b = 0$ the whole system of equations is satisfied. Otherwise they are only approximately satisfied. Figures 6 and 7 show that a is between $0.96 \div 1$ and b is between $0 \div 0.3$ for the range of ϕ and θ between $\pm 30^\circ$. This shows that the approximation is good for moderate ϕ and θ angles which occur during take-off or landing.

From the above calculations two force vectors result applying a correction in the formulation to satisfy force equilibrium.

$$\begin{aligned} F_{r_E} &= [a \quad b \quad 0]^T \mu'_r N \\ F_{s_E} &= [0 \quad 1 \quad 0]^T \mu' N \\ F_{r_E} + F_{s_E} &= [a\mu'_r N \quad \mu' N + b\mu'_r N \quad 0]^T \end{aligned} \quad (11)$$

Without considering the saturation of coefficients, the last equation gives:

$$F_{r_E} + F_{s_E} = [-F^E(x) \quad -F^E(y) \quad 0]$$

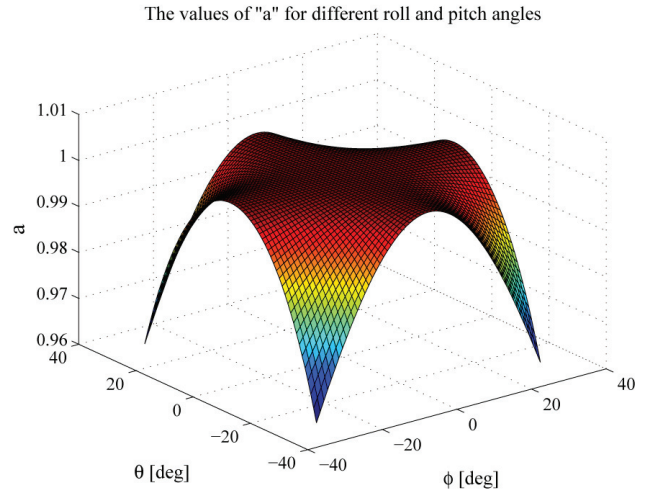


Fig. 6. 'a' parameter values against pitch and bank angles

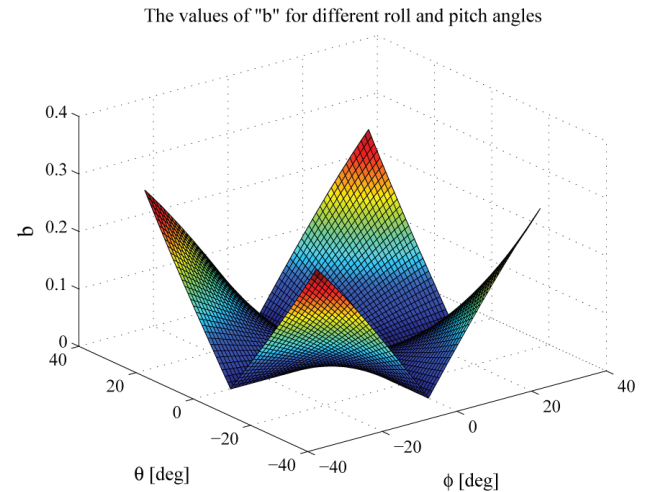


Fig. 7. 'b' parameter values against pitch and bank angles

Which is correctly the force vector opposite to the forces acting on the aircraft. Of course with the saturation, the resulting maximum ground force can be smaller, so equilibrium will not be possible.

For the yaw moment, the possible static friction coefficient is calculated irrespective of the sliding force above (it is assumed

that both the potential sliding force and yaw moment act on the A/C):

$$\mu_s'' = \frac{-M^E(z)}{cm_z \cdot N} \quad \mu_s'' = \frac{\mu_s''}{|\mu_s''|} \mu_s$$

Here, the static friction coefficient is again saturated, finally the possible equilibrium yaw moment

$$M_{z_e} = \mu_s'' cm_z \cdot N$$

STEP 10. Calculate potential (maximum possible) forces and moments from ground assuming that the aircraft moves and rotates on it.

$$a = -ssign(V^E(x)) \sqrt{\frac{\cos^2 \phi}{\sin^2 \phi \sin^2 \theta + \cos^2 \phi}}$$

$$b = \sqrt{1 - a^2}$$

if $sign(ab) \neq -sign(\phi)sign(\theta)$: $b = -b$

$$F_x = [a \quad b \quad 0] \mu_s \cdot N \quad (12)$$

$$F_y = -ssign(V^E(y)) [0 \quad 1 \quad 0] \mu_s \cdot N$$

$$M_z = -km_z \omega^E(z)$$

$$\text{if } |M_z| > M_{lim} \quad M_z = \frac{M_{lim} \cdot M_z}{|M_z|}$$

Here, the sign of aircraft X direction velocity is considered instead of the X direction force in the calculation of a because rolling friction should act opposite to the rolling direction. In the calculation of F_y the sign of the Y direction velocity is considered. The potential yaw moment is calculated from the damping coefficient and aircraft angular rate and is limited (to $M_{lim} = 5 \text{ Nm}$ in the application example).

The roll and pitch moments are calculated as follows:

$$M_x = -cm_x \phi^E - km_x \omega^E(x) \quad (13)$$

$$M_y = -cm_y \theta^E - km_y \omega^E(y)$$

STEP 11. Calculate the final forces and moments:

$$F_x = F_{r_e} + \min\left(\left[1 \quad |V^E(x)|\right]\right) (F_x - F_{r_e})$$

$$F_y = F_{s_e} + \min\left(\left[1 \quad |V^E(y)|\right]\right) (F_y - F_{s_e}) \quad (14)$$

$$M_z = M_{z_e} + \min\left(\left[1 \quad |\omega^E(z) / \omega_{lim}|\right]\right) \cdot (M_z - M_{z_e})$$

The X and Y friction forces and the yaw moment are interpolated between possible (maximum) and required (equilibrium)

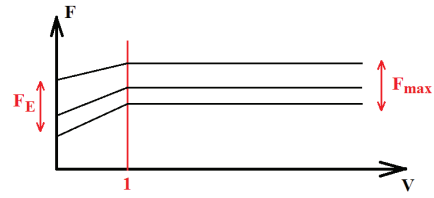


Fig. 8. Array of curves of saturated forces

values with velocity and angular velocity. The goal is to provide continuously decreasing force and moment with decreasing velocities to make the achievement of zero velocities possible. This way the simulation can stop the aircraft.

For large velocities above 1 F_x , F_y and M_z potential (maximum) forces and moment are applied (the limit yaw rate is selected as $\omega_{lim} = 0.01 \text{ rad/s}$ instead of 1). As the velocities go to zero, the final force achieves the required which means zero resultant force and so no acceleration. This is visualized in figure 8 which also shows that the equilibrium and maximum forces can vary and so, these equations describe arrays of curves.

The X and Y moments are not interpolated because they solely depend on pitch and bank angles and angular rates and so reach zero values as angles and rates reach.

The summing of all ground forces and moments and their transformation into body coord. sys. is the final step of the calculation:

$$F_G = T_{EB}^T (F_x + F_y + F_N)$$

$$M_G = T_{EB}^T \begin{bmatrix} M_x \\ M_y \\ M_z \end{bmatrix} \quad (15)$$

4 SIL simulation results

A flight test simulation was conducted in the SIL test environment originally developed by (Paw, 2009) but completed with manual RC control and the ground model. A whole flight from take-off to landing was simulated without wind disturbances. The results can be seen in figures from 9 to 12. The forces and moments are all in the body coordinate system. 'Body' means all the forces and moments acting on the aircraft without the ground forces and moments.

The figures show that the ground simulation works well. At the beginning, the aircraft stands on the ground with X and Z body and ground force components which represent the gravitational force. The Y component is zero as expected with zero roll angle. The moments are all zero.

At take-off the X body force increases showing the thrust of the engine. During take-off the X and Z body forces decrease with increasing air drag and lift force. The ground forces decrease to zero when the aircraft leaves the ground.

In the air all the body forces are approximately zero with approximately constant flight speed.

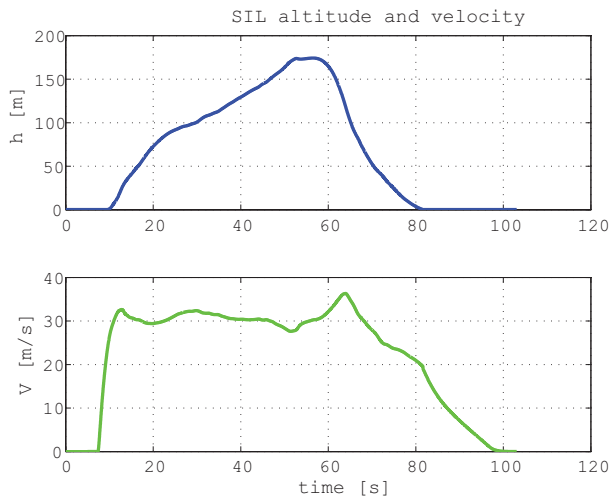


Fig. 9. Flight altitude and ground speed

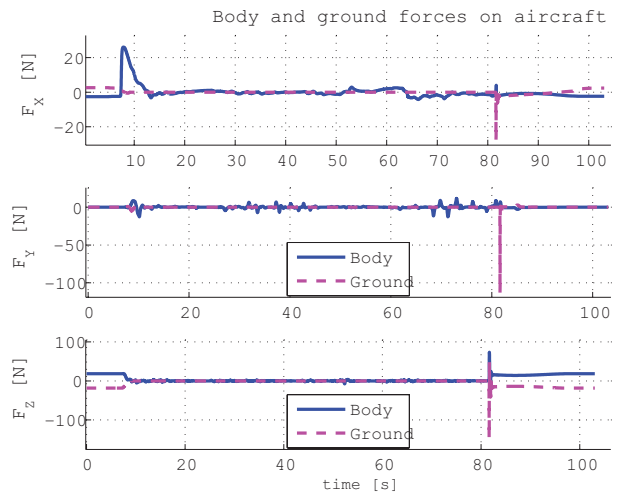


Fig. 11. Body and ground forces

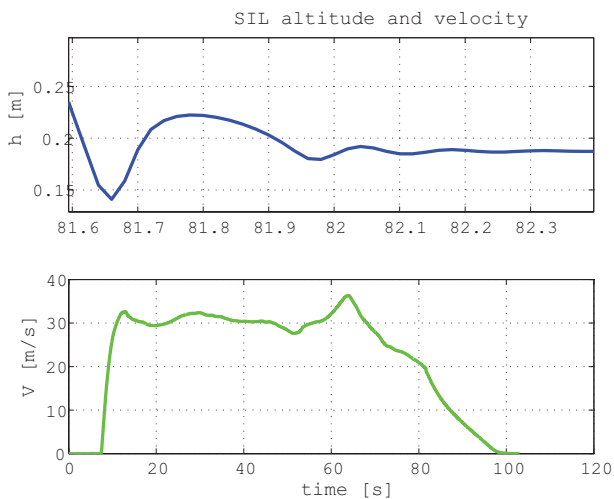


Fig. 10. Flight altitude and ground speed magnified figure

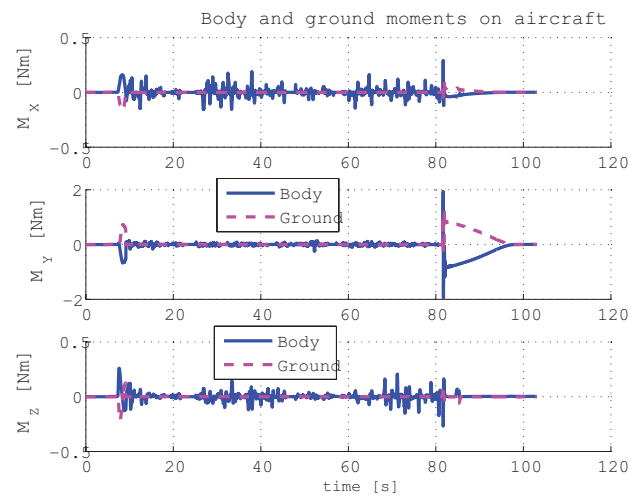


Fig. 12. Body and ground moments

At landing the Z ground force suddenly increases and this increases also the X and Y components. After some oscillations the aircraft stops and the equilibrium X, Y and Z forces occur again. The oscillations in CG height (altitude) can be seen in figure 10. The oscillation amplitude is a few cm as experienced in real flight tests also.

During take-off the ground moments compensate the body moments until the aircraft leaves the ground. In flight ground moments are zero. After landing the X and Y ground moments well balance the body moments until the speed and so the body moments decrease to zero.

5 Conclusions

In this paper a simple landing gear model was presented for small unmanned aerial vehicles. The model does not consider the braking and steering of wheels, but considers the effect of decreasing forces and moments during deceleration of aircraft.

These are scaled in a way that the aircraft stops if it reaches zero velocity and angular rate.

Software-in-the-loop simulation results present the working of the developed model. Software- and Hardware-in-the-loop simulations completed with this landing gear model were used to tune and test aircraft orientation estimation algorithms from take-off to landing in (Bauer, Bokor, 2010; Bauer, 2010; Bauer, Bokor, 2011; Bauer, 2013).

Later this model can be applied in the design and testing of auto take-off and auto landing capabilities.

Acknowledgements

The project has been supported by the Foundation for Hungarian Transportation Engineering and the HungaroControl, the Hungarian Air NAVIGATION Services Co.

References

- 1 *jsbsim groundreactions* (wiki.flightgear.org).
- 2 **Abdunabi T.**, *Modelling and Autonomous Flight Simulation of a Small Unmanned Aerial Vehicle*. Master's thesis, University of Sheffield, (August 2006).
- 3 **Barnes A. G., Yager T. J.**, *Simulation of aircraft behaviour on and close to the ground*. Technical Report 285, AGARD (January 1985).
- 4 **Bauer P.**, *Optimal tracking control for unmanned aerial vehicles*. PhD thesis, Budapest University of Technology and Economics, Budapest, Hungary, (May 2013).
- 5 **Bauer P., Bokor J.**, *Development and Hardware-in-the-Loop Testing of an Extended Kalman Filter for Attitude Estimation*. in 'Proc. of 11th IEEE International Symposium on Computational Intelligence and Informatics (CINTI 2010), Budapest, Hungary', 57–62 (2010). DOI: [10.1109/CINTI.2010.5672274](https://doi.org/10.1109/CINTI.2010.5672274)
- 6 **Bauer P., Bokor J.**, *Multi-Mode Extended Kalman Filter for Aircraft Attitude Estimation*. in 'Proc. of IFAC World Congress 2011', Milano, Italy (August 2011).
- 7 **Miranda de Almeida A. D.**, *Uav flight simulator based on esa infrastructure*. Master's thesis, Instituto Superior Técnico (2007).
- 8 **Denery T., Ghidella J. R., Mosterman P. J., Shenoy R.**, *Creating Flight Simulator Landing Gear Models Using Multidomain Modeling Tools*. Technical report, The MathWorks Inc., Natick, MA, 01760 (2006). DOI: [10.2514/6.2006-6821](https://doi.org/10.2514/6.2006-6821)
- 9 **Jung D., Tsiotras P.**, *Modeling and Hardware-in-the-Loop Simulation for a Small Unmanned Aerial Vehicle*. in 'Proceedings of AIAA Infotech@Aerospace 2007 Conference and Exhibit', AIAA, 1–13 (May 2007). DOI: [10.2514/6.2007-2768](https://doi.org/10.2514/6.2007-2768)
- 10 **Kargin V.**, *Design of an Autonomous Landing Control Algorithm for a Fixed Wing UAV*. Master's thesis, Graduate School of Natural and Applied Sciences, Middle East Technical University (October 2007).
- 11 **Khapané P.**, *Simulation of Landing Gear Dynamics and Brake-Gear Interaction*. PhD thesis, Technischen Universitaet Carolo-Wilhelmina zu Braunschweig (2007).
- 12 **Lernbeiss R., Ploechl M.**, *Simulation model of an aircraft landing gear considering elastic properties of the shock absorber*. in 'Proceedings of the Institution of Mechanical Engineers part K- Journal of Multi-body Dynamics', 221 (1), 77–86, (2007).
- 13 **Lyle K. H., Jackson K. E., Fasanella E. L.**, *Simulation of aircraft landing gears with a nonlinear dynamic finite element code*. Journal of Aircraft, 39 (1), 142–147 (2002). DOI: [10.2514/2.2908](https://doi.org/10.2514/2.2908)
- 14 **Li M., Hao X., Han X., Jia H.**, *Aircraft Flight Simulation with Landing Gear Based on Multi-Domain Modeling Technology*. in 'Proceedings of 2nd International Conference on Computer Application and System Modeling', Atlantis Press, Paris, France, 493–496 (2012). DOI: [10.2991/iccasm.2012.126](https://doi.org/10.2991/iccasm.2012.126)
- 15 **Nagy D., Gáspár P.**, *Active suspension control design for unmanned ground vehicles*. Periodica Polytechnica Transportation Engineering, 40 (1), 27–32 (2012). DOI: [10.3311/pp.tr.2012-1.05](https://doi.org/10.3311/pp.tr.2012-1.05)
- 16 **Németh B., Gáspár P.**, *Vehicle modeling for integrated control design*. Periodica Polytechnica Transportation Engineering, 38 (1), 45–51 (2010). DOI: [10.3311/pp.tr.2010-1.08](https://doi.org/10.3311/pp.tr.2010-1.08)
- 17 **Paw Y. C.**, *Synthesis and Validation of Flight Control for UAV*. PhD thesis, University of Minnesota (2009).
- 18 **Bauer P.**, *Három üzemmódú kibővített Kalman szűrők repülőgép orientációjának becslésére*. in 'Repüléstudományi Közlemények elektronikus különszám, 60 éves a szolnoki repülőtisztképzés' Szolnok, Hungary (2010).
- 19 **Dassault Systèmes SIMULIA**, *Aircraft Landing Gear Simulation using Abaqus/Explicit*. Abaqus Technology Brief (2010).
- 20 **Verzichelli G.**, *Development of an Aircraft and Landing Gears Model with Steering System in Modelica-Dymola*. in 'Proceedings of Modelica 2008' Modelica Association, 181–191 (March 2008).